

Supporting Information

Reasonable design of NIR AIEgens for fluorescence imaging and effective photothermal/photodynamic cancer therapy

Hongsen Wang,^{ac} Yu Wang,^{ac} Zhaohui Zheng,^a Fang Yang,^{*bd} Xiaobin Ding,^{*a} and Aiguo Wu,^{*bd}

^a*Chengdu Institute of Organic Chemistry, Chinese Academy of Sciences, Chengdu, 610041, P.R. China. E-mail: xbding@cioc.ac.cn*

^b*Cixi Institute of Biomedical Engineering, International Cooperation Base of Biomedical Materials Technology and Application, Chinese Academy of Science (CAS) Key Laboratory of Magnetic Materials and Devices and Zhejiang Engineering Research Center for Biomedical Materials, Ningbo Institute of Materials Technology and Engineering, CAS, Ningbo 315201, P.R. China. E-mail: yangf@nimte.ac.cn, aiguo@nimte.ac.cn*

^c*University of Chinese Academy of Sciences, Beijing, 100049, P.R. China*

^d*Advanced Energy Science and Technology Guangdong Laboratory, Huizhou 516000, P.R. China*

Photothermal performance measurement ^[S1]

The DMSO solution of PTC-S-TPA, PTC-SS-TPA, TCF-S-TPA or TCF-SS-TPA at a concentration of 100 μM was irradiated with a 660 nm laser (1 W/cm^2) for 10 minutes. The temperature is recorded every 10 seconds and the corresponding infrared thermal images were acquired. The corresponding nanoparticles (25 μM) were similarly operated to evaluate the photothermal performance in aqueous solutions. Pure DMSO and pure water under the same conditions were used as controls.

Singlet oxygen detection of nanoparticles ^[S2]

The ethanol solution of DPBF (20 μM , 2mL) was added to the aqueous solution of PTC-S-TPA, PTC-SS-TPA, TCF-S-TPA or TCF-SS-TPA NPs (25 μM , 1 mL). Then, the sample was irradiated with a 660 nm laser (0.3 W/cm^2), and the absorption at 410 nm is measured every 2 minutes by a UV-vis spectrophotometer.

Photothermal conversion efficiency measurement of TCF-SS-TPA NPs ^[S2]

1mL TCF-SS-TPA NPs aqueous solution was irradiated with a 660 nm laser (1 W/cm^2) for 10 minutes. After reaching the platform temperature, the solution was naturally cooled to room temperature and record the temperature with IR thermal camera. Deionized water of the same volume was used as control. The photothermal conversion efficiency (η) is calculated by the following formula:

$$\eta = \frac{hs(T_{\max} - T_{\text{surr}}) - Q_0}{I(1 - 10^{-A})}$$

$$hs = \frac{\sum m_i C_{P_i}}{\tau_s}$$

$$\tau_s = \frac{t}{-\ln \theta}$$

$$\theta = \frac{T - T_{\text{surr}}}{T_{\max} - T_{\text{surr}}}$$

$$Q_0 = hs(T_{\max} - T_{\text{surr}})$$

Intracellular tracking ^[S1]

4T1 cell line was grown in a 1640 culture medium containing 1% antibiotics (penicillin-streptomycin) and 10% FBS at 37 °C and 5% CO_2 in a humidified environment. 4T1 cells were seeded in a glass bottom dish at an appropriate density and cultured for 24 hours. The cells were then incubated with fresh medium containing TCF-SS-TPA NPs (TCF-SS-TPA, 1.2 $\mu\text{g}/\text{mL}$) for 3 hours, washed with PBS, and then costained with Hoechst 33342 for 30

minutes. Afterwards, the samples were washed with PBS and imaged by CLSM to study the subcellular localization of TCF-SS-TPA NPs. Conditions: excitation wavelength: 405 nm for Hoechst 33342 and 552 nm for TCF-SS-TPA NPs; emission filter: 415-485 nm for Hoechst 33342 and 650-750 nm for TCF-SS-TPA NPs.

Phototoxicity test ^[S1]

4T1 cells were seeded in a 96-well plate at a density of 1×10^4 cells/well, and then cultured for 24 hours. The medium was replaced with a new medium with different concentrations of TCF-SS-TPA NPs. After incubating for 12 hours, the cells were irradiated with a 660nm laser for 5 minutes. At the same time, the same operation was performed without laser irradiation. After continuing the incubation for 12 hours, the medium was removed. The cells were washed with PBS, and then incubated with fresh serum-free medium containing 10% CCK-8 for 2 hours in the dark. Finally, the absorbance of the product was measured at a wavelength of 450 nm by a microplate reader. The relative cell viability was calculated according to the previous literature method. ^[S1]

Density functional theory calculations

The initial structure of the compound was constructed using ChemDraw, the MM2 module in Chem3D was used to minimize the energy of all compound structures. Afterwards, the Gaussian16 program package was used to optimize the structure without any symmetry constraints to obtain a better compound geometric structure. Finally, the SMD solvent model was used in the CH_2Cl_2 medium, and the density functional theory (DFT) The B3LYP method is further optimized at the 6-31G(d) basis set level, until the Hessian matrix analysis has no false frequency.

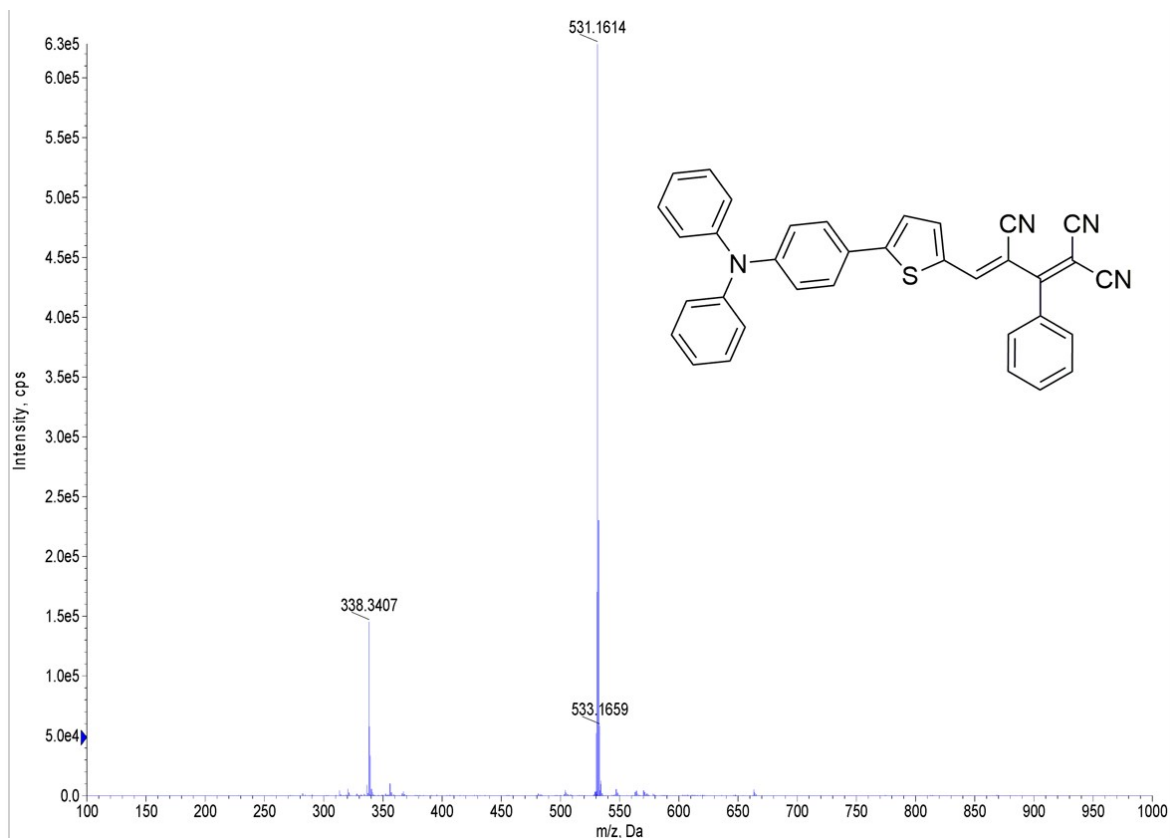


Fig. S3. TOF-MS spectrum of PTC-S-TPA

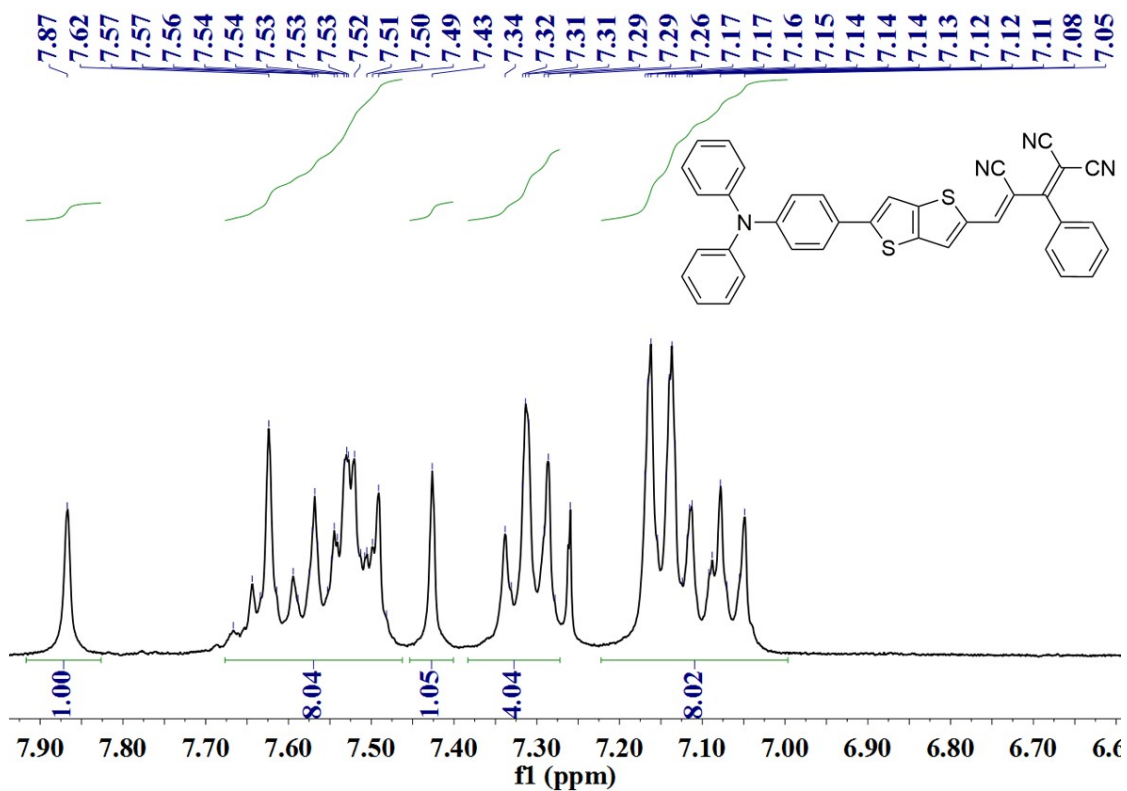


Fig. S4. ¹H NMR spectra of PTC-SS-TPA in CDCl₃.

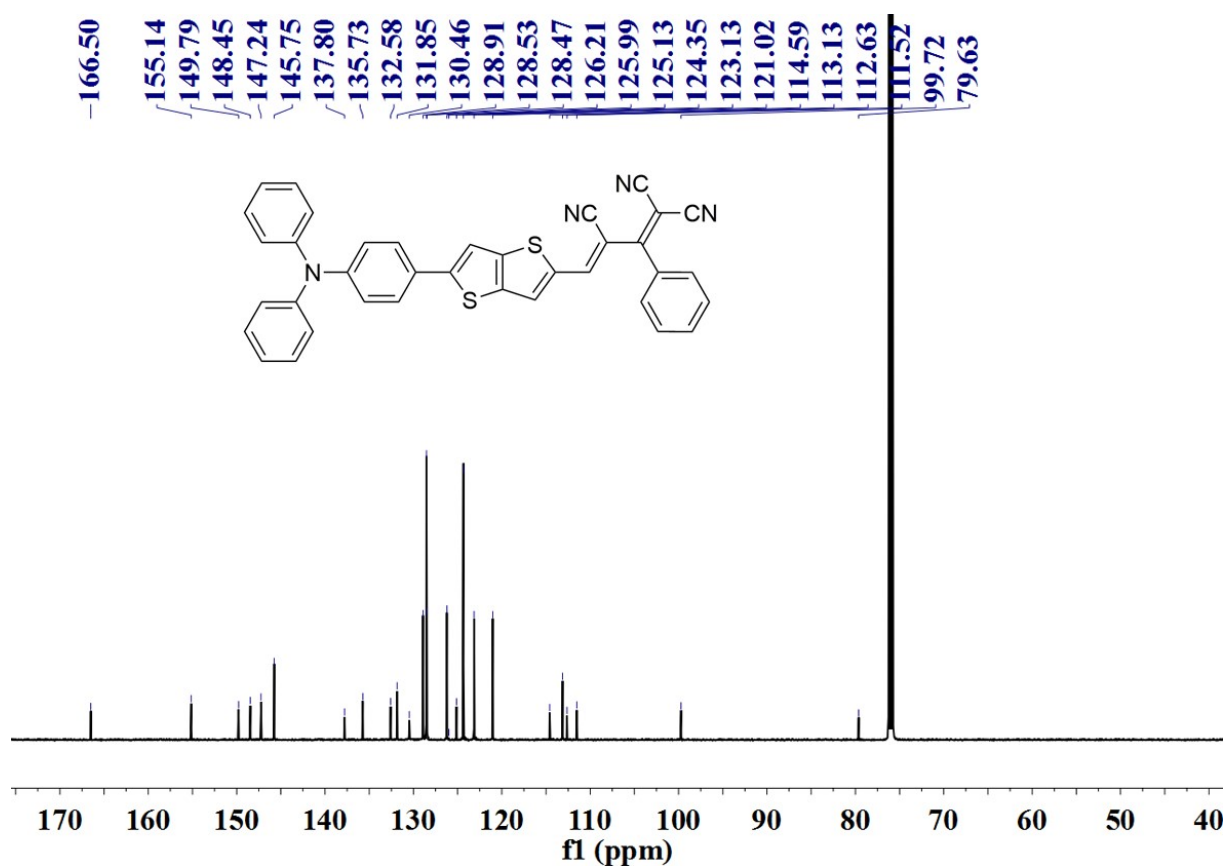


Fig. S5. ¹³C NMR spectra of PTC-SS-TPA in CDCl₃.

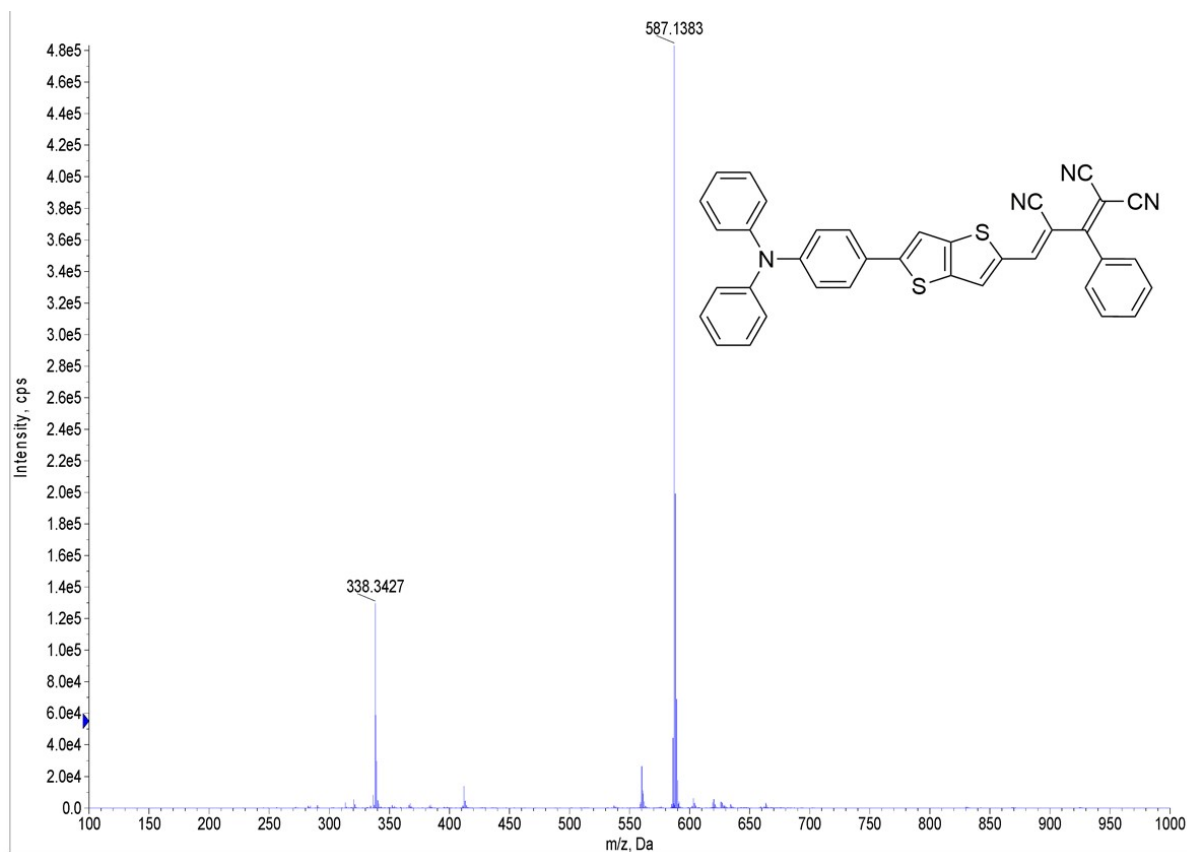


Fig. S6. TOF-MS spectrum of PTC-SS-TPA

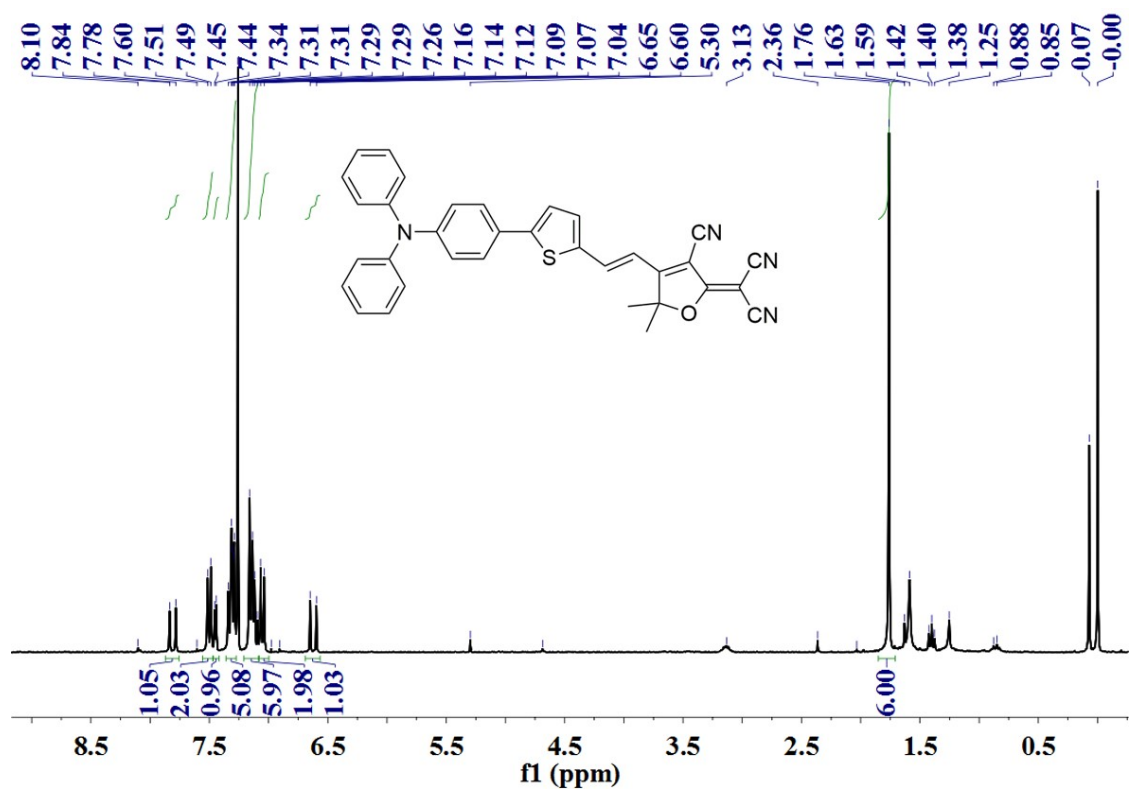


Fig. S7. ^1H NMR spectra of TCF-S-TPA in CDCl_3 .

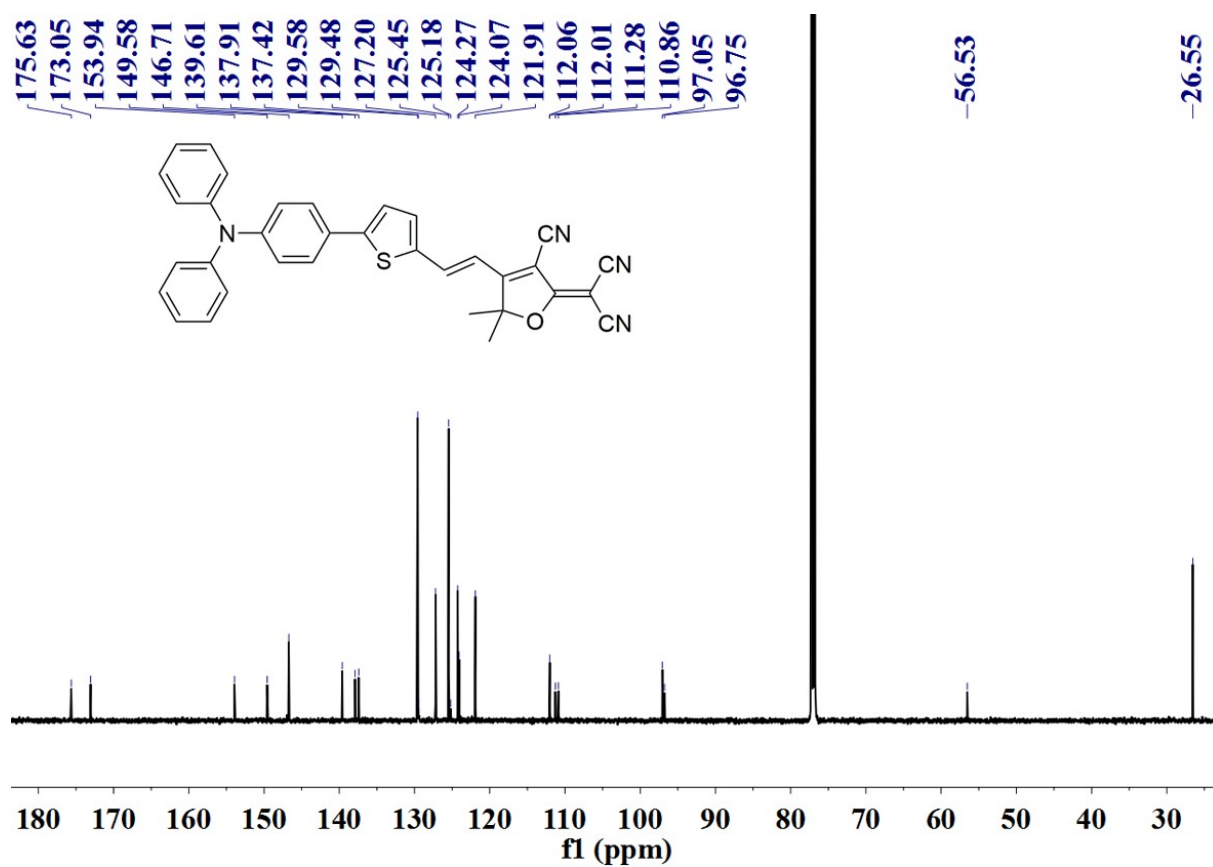


Fig. S8. ^{13}C NMR spectra of TCF-S-TPA in CDCl_3 .

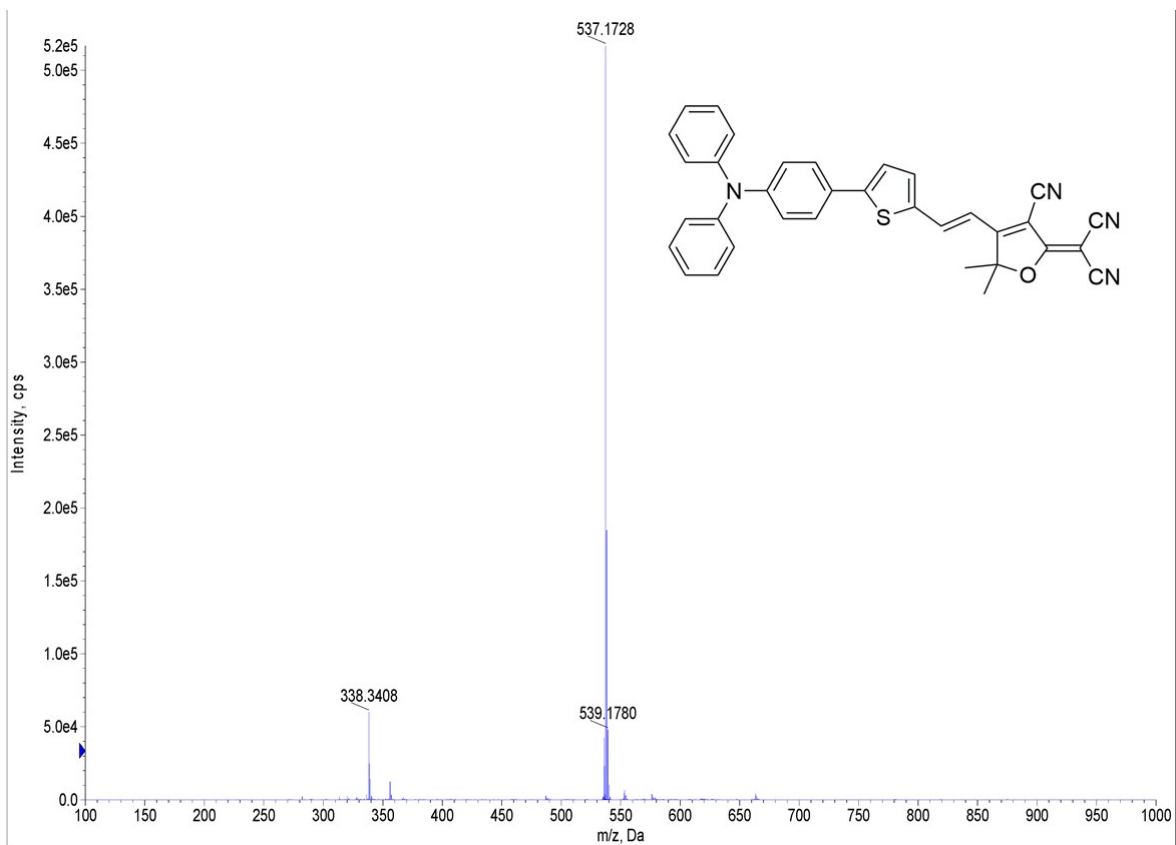


Fig. S9. TOF-MS spectrum of TCF-S-TPA

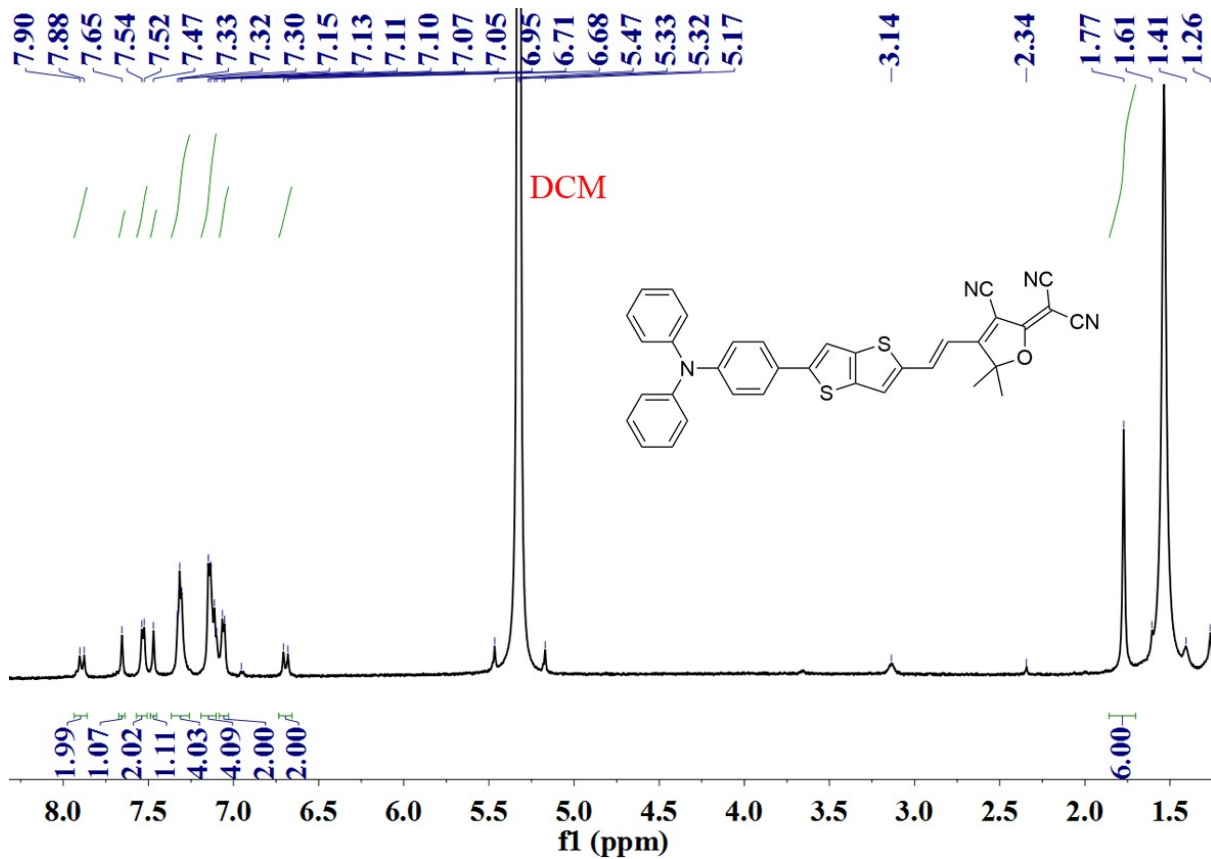


Fig. S10. ^1H NMR spectra of TCF-SS-TPA in CD_2Cl_2 .

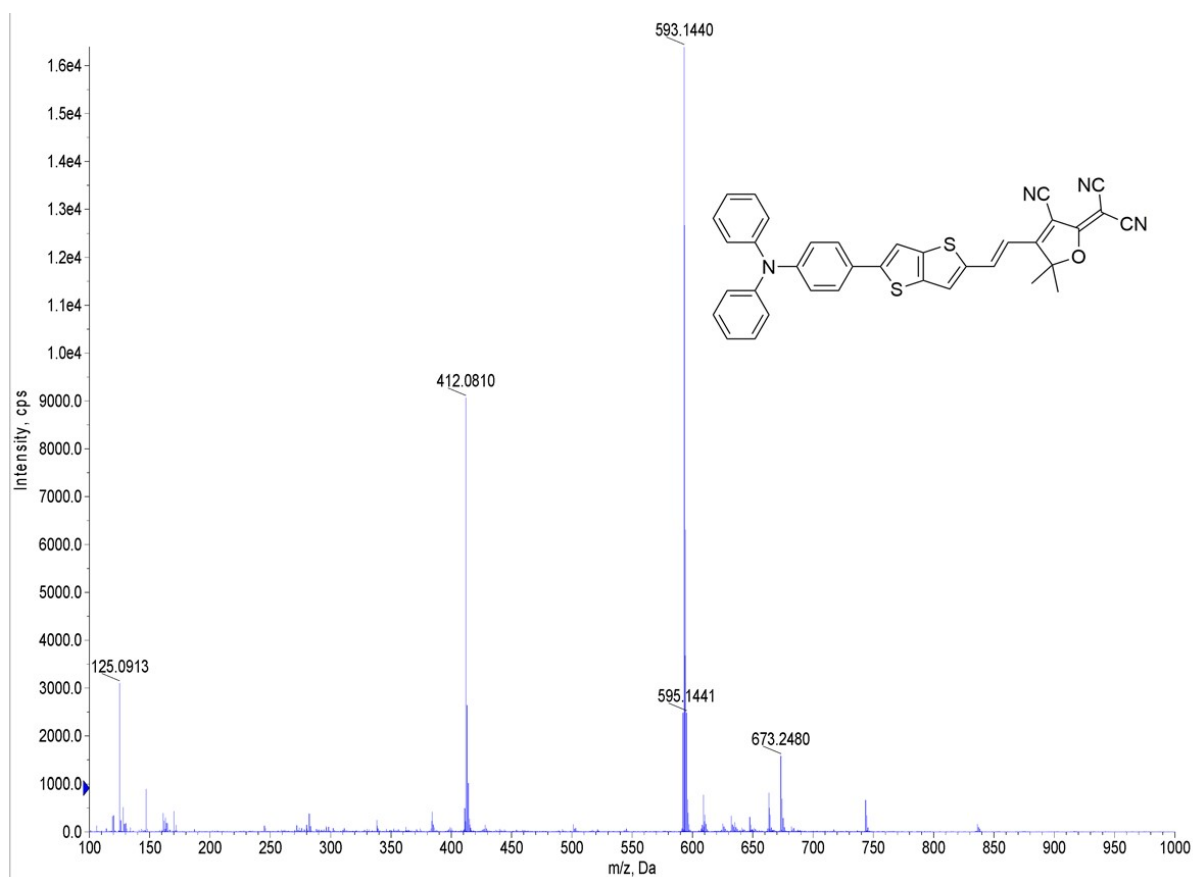


Fig. S11. TOF-MS spectrum of TCF-SS-TPA

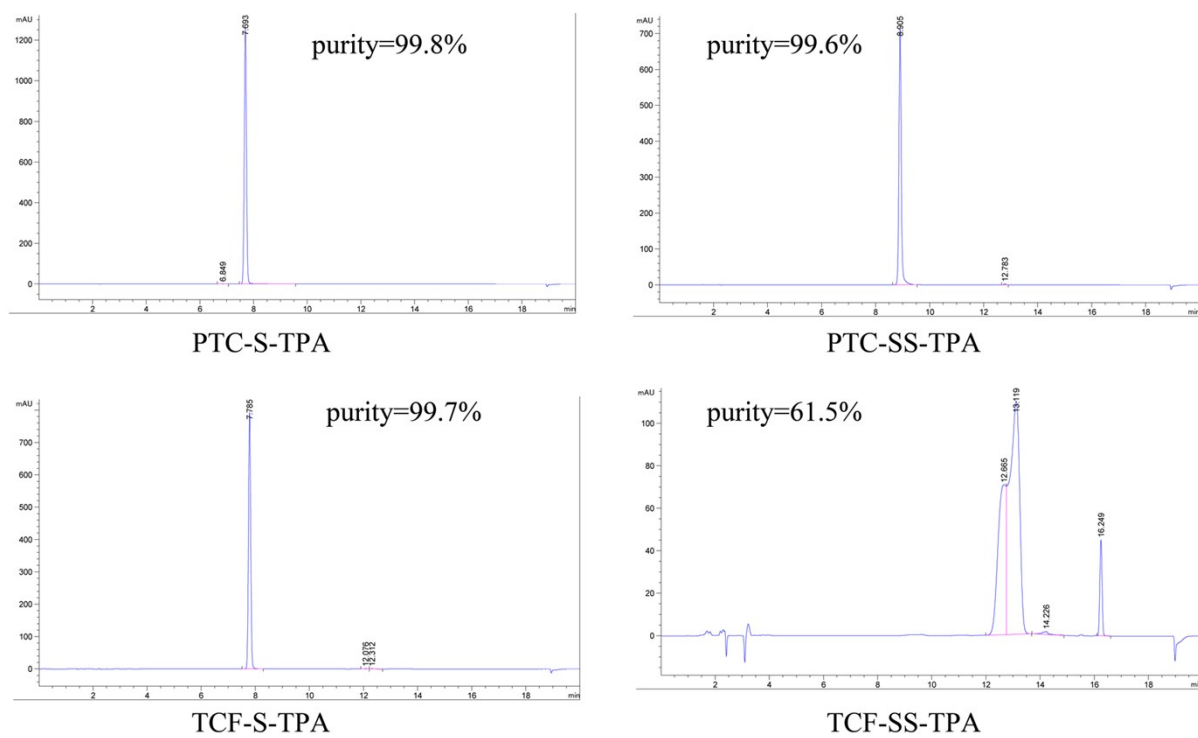


Fig. S12. HPLC spectrum of PTC-S-TPA, PTC-SS-TPA, TCF-S-TPA and TCF-SS-TPA

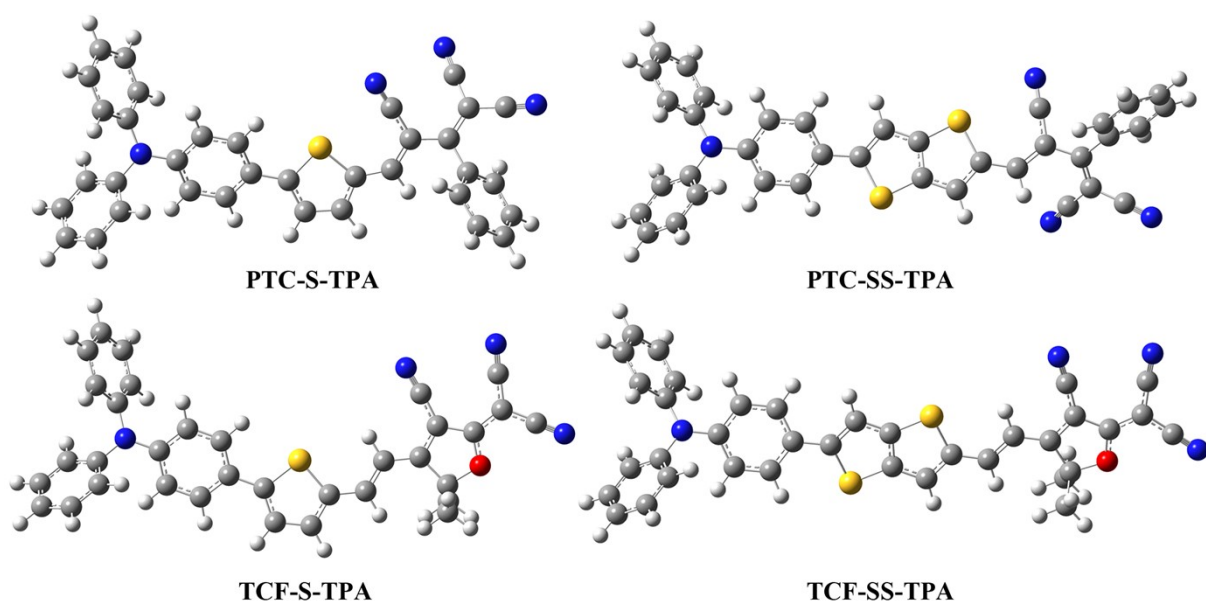


Fig. S13. The optimized molecular structure by DFT method

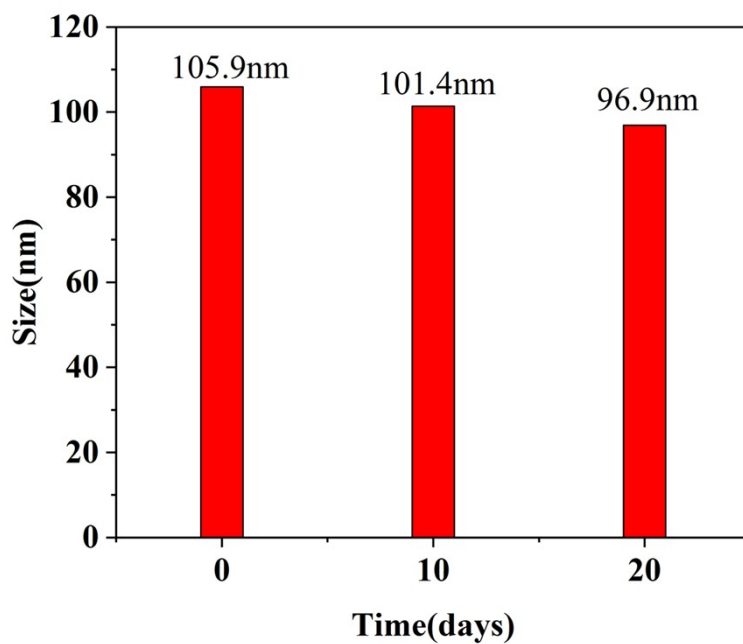


Fig. S14. Average size change of TCF-SS-TPA NPs at room temperature for 20 days.

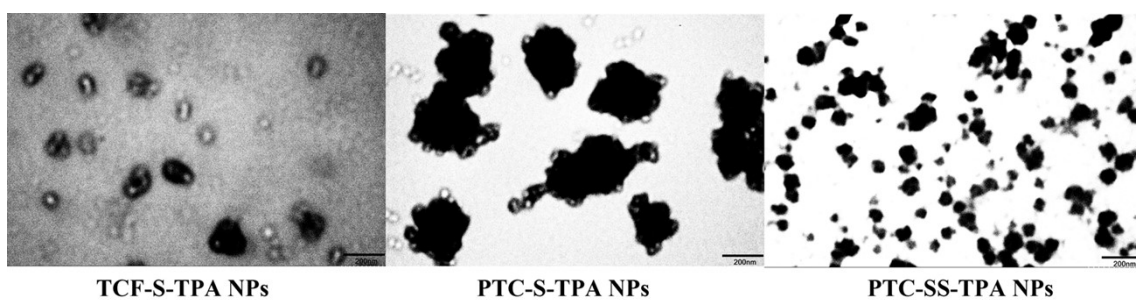


Fig. S15. TEM image of TCF-S-TPA NPs, PTC-S-TPA NPs and PTC-SS-TPA NPs.

Aggregation-induced emission (AIE) performance

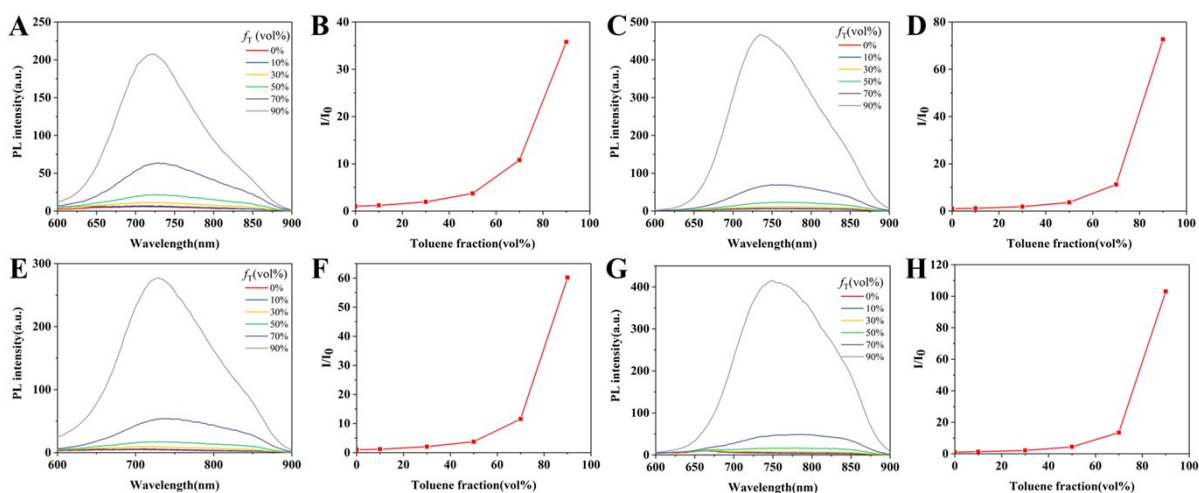


Fig. S16. PL spectra of (A) PTC-S-TPA, (C) TCF-S-TPA, (E) PTC-SS-TPA and (G) TCF-SS-TPA in DMSO/toluene with different toluene fractions (f_T); Plots of the relative emission intensity of (B) PTC-S-TPA, (D) TCF-S-TPA, (F) PTC-SS-TPA, and (H) TCF-SS-TPA *versus* toluene fraction. I_0 and I are the peak values of photoluminescence intensities of AIEgens (10 μ M) in DMSO and DMSO/toluene mixtures, respectively.

Photostability comparison of TCF-SS-TPA NPs with MB and ICG

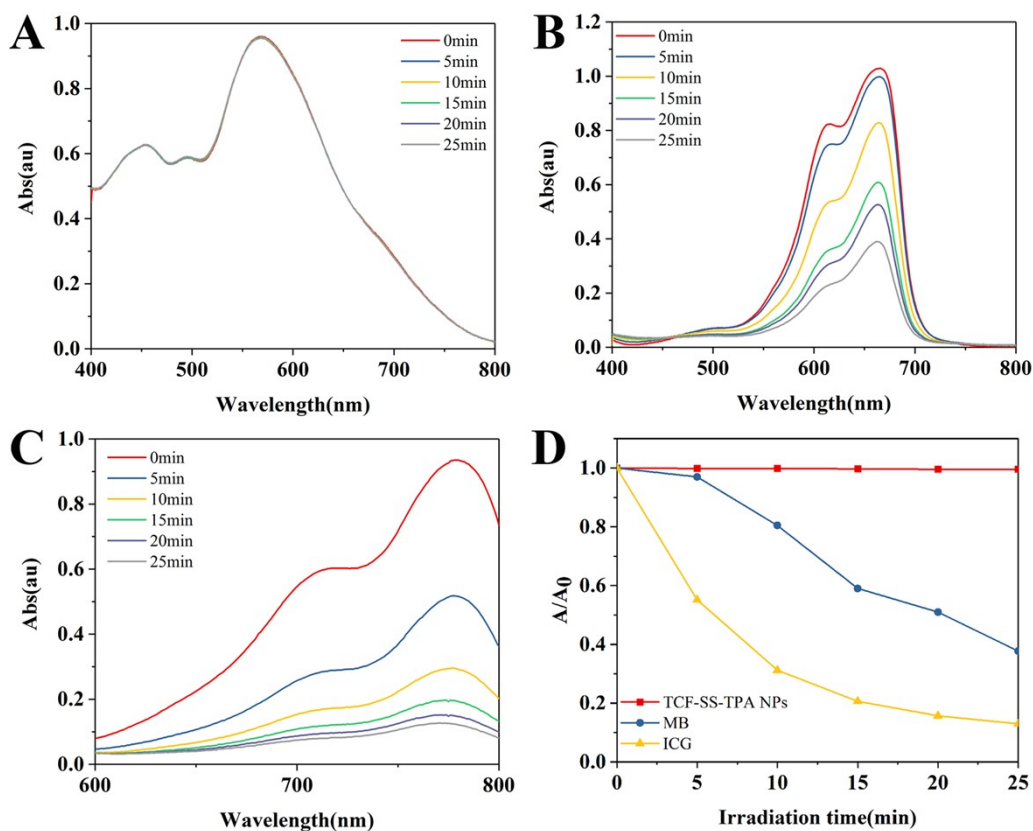


Fig. S17. Absorption spectra of materials under 660 nm (0.5W/cm²) laser at different irradiation time. A) TCF-SS-TPA NPs, B) MB, C) ICG, D) Absorption peak of materials under 660 nm laser at different irradiation time.

Singlet oxygen analysis of nanoparticles

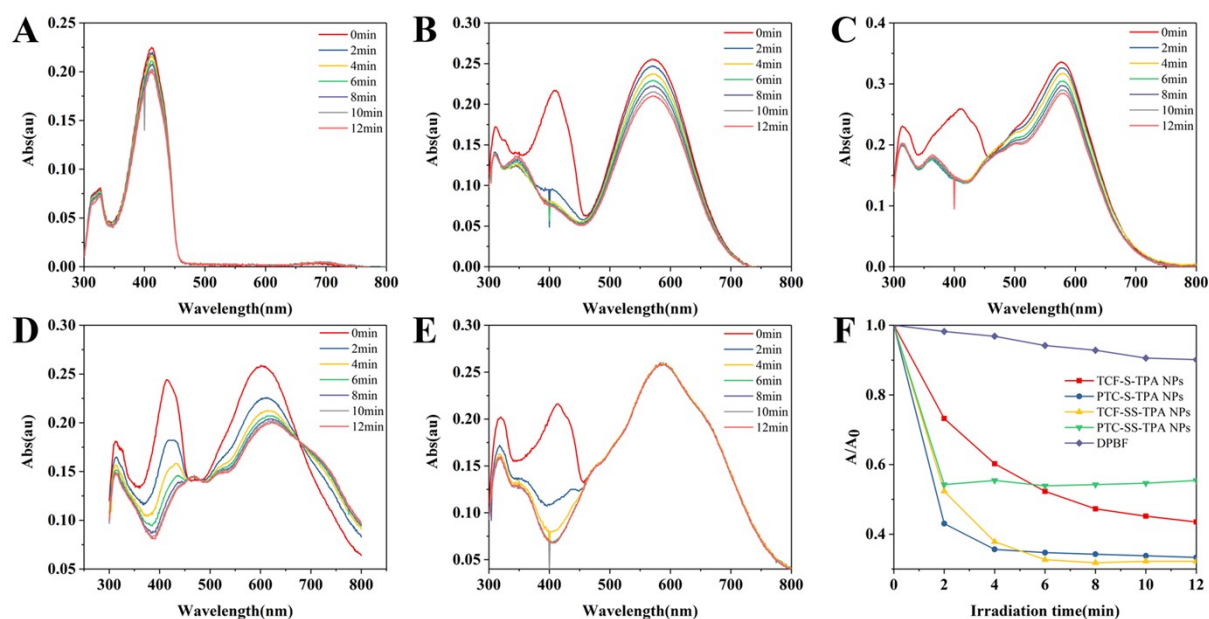


Fig. S18. Absorption spectra of the mixed aqueous solution of nanoparticle and DPBF under 660 nm ($0.3\text{W}/\text{cm}^2$) laser at different irradiation time. A) only DPBF, B) DPBF and PTC-S-TPA NPs, C) DPBF and PTC-SS-TPA NPs, D) DPBF and TCF-S-TPA NPs, E) DPBF and TCF-SS-TPA NPs, F) Absorption at 410 nm of DPBF with nanoparticles under 660 nm laser at different irradiation time.

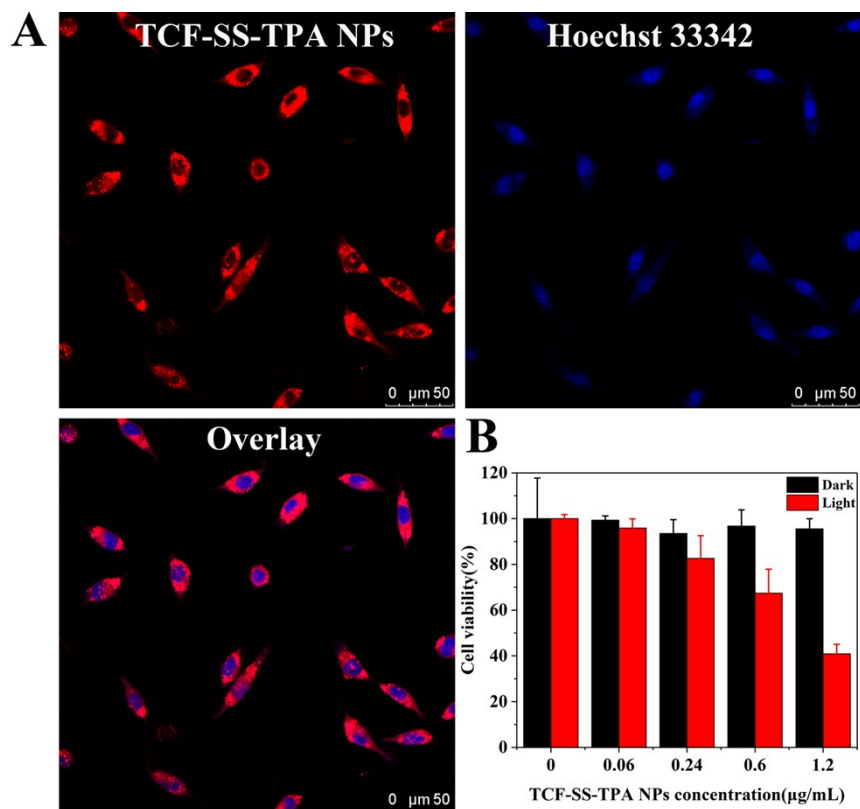


Fig. S19. The dark toxicity, light toxicity and CLSM imaging in L929 cells.

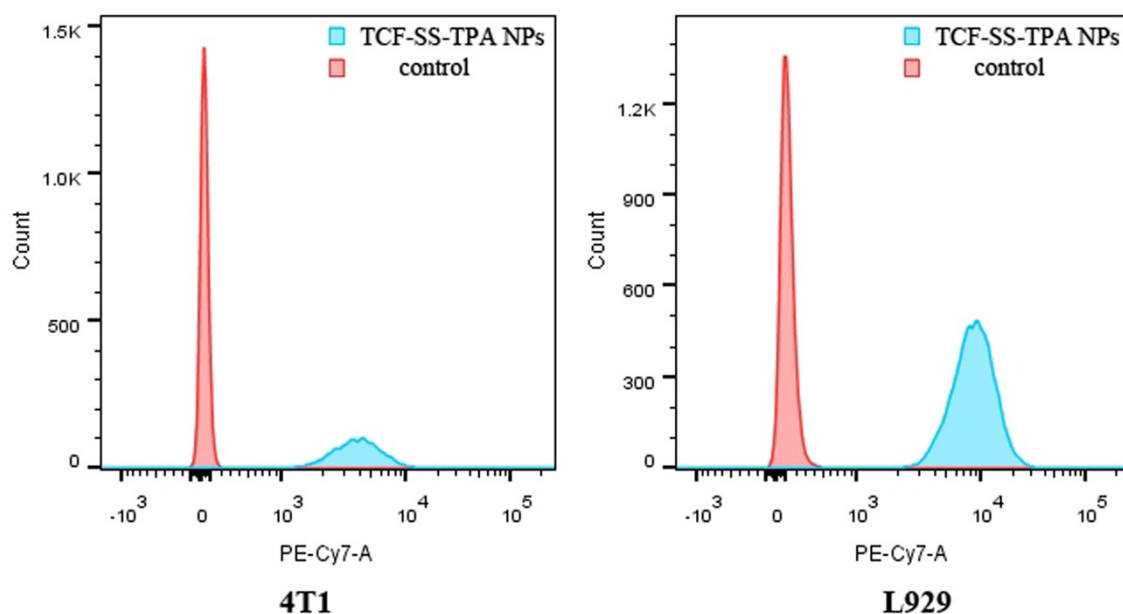


Fig. S20. The flow cytometry analysis of 4T1 and L929 cell uptake.

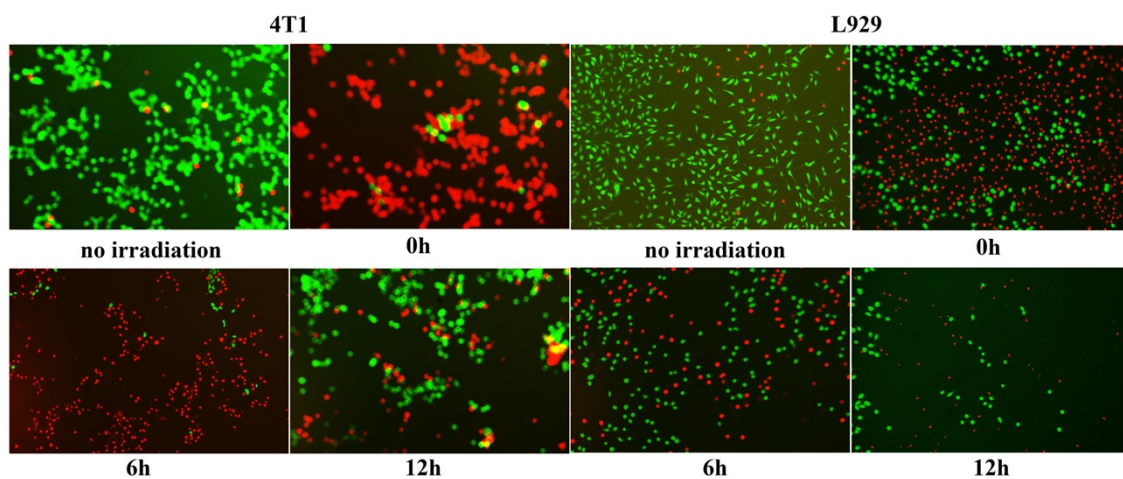


Fig. S21. Live-dead cell staining at different times after 5min of 660nm laser irradiation.

References:

- [S1] Z. Zhang, W. Xu, M. Kang, H. Wen, H. Guo, P. Zhang, L. Xi, K. Li, L. Wang, D. Wang and B. Z. Tang, *Adv. Mater.*, 2020, 2003210.
- [S2] Q. Wang, Y. Dai, J. Xu, J. Cai, X. Niu, L. Zhang, R. Chen, Q. Shen, W. Huang and Q. Fan, *Adv. Funct. Mater.*, 2019, **29**, 1901480.